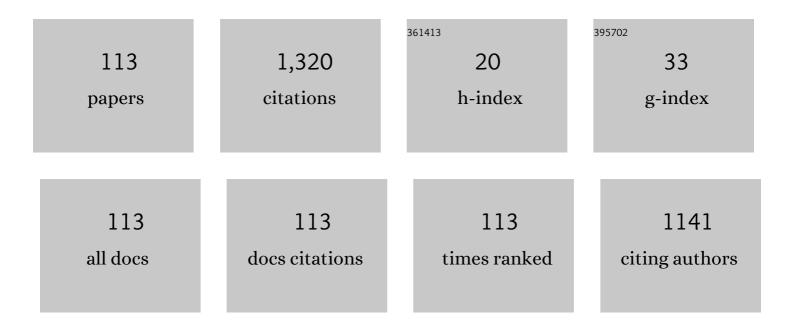
List of Publications by Year in descending order

Source: https://exaly.com/author-pdf/517820/publications.pdf Version: 2024-02-01



MASAHIKO MORI

#	Article	IF	CITATIONS
1	Switching dynamics of silicon waveguide optical modulator driven by photothermally induced metal-insulator transition of vanadium dioxide cladding layer. Optics Express, 2020, 28, 37188.	3.4	12
2	Silicon waveguide optical modulator driven by metal–insulator transition of vanadium dioxide cladding layer. Optics Express, 2019, 27, 4147.	3.4	31
3	45-degree curved micro-mirror for vertical optical I/O of silicon photonics chip. Optics Express, 2019, 27, 19749.	3.4	16
4	High density optical card edge connector for polymer optical waveguide on printed circuit board. , 2018, , .		2
5	Mirror-based polarization-insensitive broadband vertical optical coupling for Si waveguide. Japanese Journal of Applied Physics, 2017, 56, 090302.	1.5	7
6	Controlled initial orientation of liquid crystals in silicon optical switches with a groove array. , 2017, , .		0
7	Compact and low-loss liquid crystal loaded Mach-Zehnder optical switch based on Si wire waveguide. IEICE Electronics Express, 2017, 14, 20170110-20170110.	0.8	1
8	Ultrahigh-Q photonic crystal nanocavities fabricated by CMOS process technologies. Optics Express, 2017, 25, 18165.	3.4	41
9	Mirror-based surface optical input/output technology with precise and arbitrary coupling angle for silicon photonic application. Japanese Journal of Applied Physics, 2017, 56, 04CH04.	1.5	0
10	Low-Loss Characteristics of a Multimode Polymer Optical Waveguide at 1.3 um Wavelength on an Electrical Hybrid LSI Package Substrate. , 2016, , .		5
11	Raman scattering in hydrogenated amorphous silicon waveguides at telecommunication wavelengths. , 2016, , .		0
12	Vertically Curved Si Waveguide Coupler with Low Loss and Flat Wavelength Window. Journal of Lightwave Technology, 2016, 34, 1567-1571.	4.6	23
13	Interlayer Polarization Beam Splitter Based on Asymmetrical Si Wire Directional Coupler. IEEE Photonics Technology Letters, 2016, 28, 1545-1548.	2.5	7
14	In-plane switching mode-based liquid-crystal hybrid Si wired Mach–Zehnder optical switch. Japanese Journal of Applied Physics, 2016, 55, 118003.	1.5	7
15	Broadband and Polarization-Independent Efficient Vertical Optical Coupling With 45° Mirror for Optical I/O of Si Photonics. Journal of Lightwave Technology, 2016, 34, 3012-3018.	4.6	8
16	25-Gb/s Operation of a Polymer Optical Waveguide on an Electrical Hybrid LSI Package Substrate With Optical Card Edge Connector. Journal of Lightwave Technology, 2016, 34, 3006-3011.	4.6	10
17	Broadband and Polarization-Independent Efficient Vertical Optical Coupling With 45° Mirror for Optical I/O of Si Photonics. Journal of Lightwave Technology, 2016, 34, 978-984.	4.6	8
18	CMOS-compatible Vertical Si-waveguide Coupler Fabricated by Ion Implantation. , 2016, , .		1

#	Article	IF	CITATIONS
19	Hydrogenated amorphous silicon photonic devices on synthetic quartz glass substrate. , 2015, , .		Ο
20	A method enabling height-control of chips for edge-emitting laser stacking. Japanese Journal of Applied Physics, 2015, 54, 04DB02.	1.5	0
21	Quantum Dot Laser for a Light Source of an Athermal Silicon Optical Interposer. Photonics, 2015, 2, 355-364.	2.0	5
22	Vertical silicon waveguide coupler bent by ion implantation. Optics Express, 2015, 23, 29449.	3.4	33
23	A 25-Gbps operation of polymer-based optical and electrical hybrid LSI package substrate with optical card edge connector. , 2015, , .		3
24	Broadband and polarization-independent efficient vertical optical coupling with Si integrated 45 degree mirror. , 2015, , .		1
25	Low-loss and low wavelength-dependence vertical interlayer transition for 3D silicon photonics. Optics Express, 2015, 23, 18602.	3.4	23
26	Spot-size converter with a SiO_2 spacer layer between tapered Si and SiON waveguides for fiber-to-chip coupling. Optics Express, 2015, 23, 21287.	3.4	25
27	Multi-channel Hybrid Integrated Light Source for Ultra-high-bandwidth Optical Interconnections and Its Structural Optimization for Low Power Consumption by Considering Thermal Interference between LD Arrays. Transactions of the Japan Institute of Electronics Packaging, 2014, 7, 94-103.	0.4	6
28	Over-1000-channel hybrid integrated light source with laser diode arrays on a silicon waveguide platform for ultra-high-bandwidth optical interconnections. , 2014, , .		3
29	Carrier injection refractive index changes in low-temperature grown silicon waveguide. , 2014, , .		2
30	Demonstration of 25-Gbps optical data links on silicon optical interposer using FPGA transceiver. , 2014, , .		4
31	Athermal silicon optical interposers with quantum dot lasers operating from 25 to 125°C. Electronics Letters, 2014, 50, 1377-1378.	1.0	Ο
32	Silicon knife-edge taper fiber coupler using CMOS backend compatible process. , 2014, , .		1
33	Optical-Time-Division Demultiplexing of 172 Gb/s to 43 Gb/s in a-Si:H Waveguides. IEEE Photonics Technology Letters, 2014, 26, 426-429.	2.5	4
34	Sub-1 dB/cm submicrometer-scale amorphous silicon waveguide for backend on-chip optical interconnect. Optics Express, 2014, 22, 4779.	3.4	39
35	Multichannel and high-density hybrid integrated light source with a laser diode array on a silicon optical waveguide platform for interchip optical interconnection. Photonics Research, 2014, 2, A19.	7.0	32
36	Multi-channel and high-density hybrid integrated light source by thermal management for low power consumption for ultra-high bandwidth optical interconnection. , 2014, , .		2

#	Article	IF	CITATIONS
37	A Hybrid Integrated Light Source on a Silicon Platform Using a Trident Spot-Size Converter. Journal of Lightwave Technology, 2014, 32, 1329-1336.	4.6	152
38	Highly transpearent submicrometer-sclae amorphous silicon waveguide for backend optical interconnect. , 2014, , .		0
39	Demonstration of over 1000-Channel Hybrid Integrated Light Source for Ultra-High Bandwidth Interchip Optical Interconnection. , 2014, , .		5
40	Hybrid integration technology of laser source with laser diode arrays on silicon optical waveguide platform by flip-chip bonding for silicon photonics. , 2013, , .		3
41	Compact and phase-error-robust multilayered AWG-based wavelength selective switch driven by a single LCOS. Optics Express, 2013, 21, 17131.	3.4	17
42	Observation of spontaneous Raman scattering in hydrogenated amorphous silicon wire waveguide at 1.55 µm. Electronics Letters, 2013, 49, 610-612.	1.0	0
43	Silicon knife-edge taper waveguide for ultralow-loss spot-size converter fabricated by photolithography. Applied Physics Letters, 2013, 102, .	3.3	44
44	First demonstration of a hybrid integrated light source on a Si platform using a quantum dot laser under wide temperature range. , 2013, , .		2
45	2.2 pJ/bit operation of hybrid integrated light source on a silicon optical interposer for optical interconnection. , 2013, , .		4
46	MEMS mirror with slot structures suitable for flexible-grid WSS. IEICE Electronics Express, 2013, 10, 20120924-20120924.	0.8	5
47	Pattern-effect-free all-optical wavelength conversion using a hydrogenated amorphous silicon waveguide with ultra-fast carrier decay. Optics Letters, 2012, 37, 1382.	3.3	37
48	Basic Study of Coupling on Three-Dimensional Crossing of Si Photonic Wire Waveguide for Optical Interconnection on Inter or Inner Chip. Japanese Journal of Applied Physics, 2012, 51, 04DG12.	1.5	4
49	Demonstration of 125-Gbps optical interconnects integrated with lasers, optical splitters, optical modulators and photodetectors on a single silicon substrate. Optics Express, 2012, 20, B256.	3.4	53
50	High-density hybrid integrated light sources for photonics-electronics convergence system. , 2012, , .		0
51	Nanometer-scale thickness control of amorphous silicon using isotropic wet-etching and low loss wire waveguide fabrication with the etched material. Applied Physics Letters, 2012, 100, 251108.	3.3	23
52	Ultranarrow Silicon Inverse Taper Waveguide Fabricated with Double-Patterning Photolithography for Low-Loss Spot-Size Converter. Applied Physics Express, 2012, 5, 052202.	2.4	22
53	Plasma deposited µc-Si:H wire waveguide. , 2012, , .		0
54	Analysis of vertical coupling between a 2D photonic crystal cavity and a hydrogenated-amorphous-silicon-wire waveguide. Photonics and Nanostructures - Fundamentals and Applications, 2012, 10, 287-295.	2.0	3

#	Article	IF	CITATIONS
55	Transmission Characteristics of Hydrogenated Microcrystalline Silicon Wire Waveguide at a Wavelength of 1.55 \$mu\$m. Applied Physics Express, 2012, 5, 082501.	2.4	4
56	Multi-Channel and High-Density Hybrid Integrated Light Source on Silicon Optical Waveguide Platform. , 2012, , .		3
57	Multi-Channel and High-Density Hybrid Integrated Light Source on Silicon Optical Waveguide Platform. , 2012, , .		1
58	Basic Study of Coupling on Three-Dimensional Crossing of Si Photonic Wire Waveguide for Optical Interconnection on Inter or Inner Chip. Japanese Journal of Applied Physics, 2012, 51, 04DG12.	1.5	2
59	Fine thickness control of amorphous silicon by wet-etching for low loss wire waveguide. , 2011, , .		1
60	High density hybrid integrated light source with a laser diode array on a silicon optical waveguide platform for inter-chip optical interconnection. , 2011, , .		29
61	Phase error compensation for multilayered AWG in LCOS-based WSS. IEICE Electronics Express, 2011, 8, 2054-2060.	0.8	2
62	Reduced Lasing Threshold in Thiophene/Phenylene Co-Oligomer Crystalline Microdisks. Applied Physics Express, 2010, 3, 012702.	2.4	20
63	Fast aberration-correcting algorithm for an SLM-based optical switch. IEICE Electronics Express, 2010, 7, 1728-1734.	0.8	2
64	Microdisk lasers and field effect transistors of thiophene/phenylene co-oligomers by using high temperature deposition method. Organic Electronics, 2010, 11, 1192-1198.	2.6	27
65	Hydrogenated Amorphous Silicon Carbide Optical Waveguide for Telecommunication Wavelength Applications. Applied Physics Express, 2010, 3, 122201.	2.4	20
66	Highly stacked InGaAs quantum dot structures grown with two species of As. Journal of Vacuum Science and Technology B:Nanotechnology and Microelectronics, 2010, 28, C3C4-C3C8.	1.2	19
67	Four-wave mixing in hydrogenated amorphous silicon waveguides at 1.55 µm. , 2010, , .		Ο
68	Design of two-dimensional photonic crystal nanocavities with low-refractive-index material cladding. Journal of Optics (United Kingdom), 2010, 12, 015108.	2.2	4
69	Analysis of two-dimensional photonic crystal L-type cavities with low-refractive-index material cladding. Journal of Optics (United Kingdom), 2010, 12, 075101.	2.2	14
70	Highly Stacked and High-Quality Quantum Dots Fabricated by Intermittent Deposition of InGaAs. Japanese Journal of Applied Physics, 2010, 49, 030211.	1.5	24
71	Ultrafast nonlinear effects in hydrogenated amorphous silicon wire waveguide. Optics Express, 2010, 18, 5668.	3.4	99
72	Miniband formation in InGaAs quantum dot superlattice. Applied Physics Letters, 2010, 97, .	3.3	41

#	Article	IF	CITATIONS
73	Ultra low-power and compact photonic crystal optical switch controlled by micro-heater directly attached on PhC layer. , 2009, , .		0
74	Low threshold current operation of 1.3 µm Quantum Dots Laser with high mirror loss structure. , 2009, , .		0
75	Laser-plasma scanning 3D display for putting digital contents in free space. , 2008, , .		29
76	Spectral interferometric optical coherence tomography with nonlinear β-barium borate time gating. Optics Letters, 2002, 27, 403.	3.3	22
77	Smart pixels in a focal-plane image compression system. Optics and Laser Technology, 2002, 34, 429-437.	4.6	Ο
78	Phase-resolved correlation and its application to analysis of low-coherence interferograms. Optics Letters, 2001, 26, 90.	3.3	9
79	Analysis of spatiotemporal coupling in a femtosecond pulse shaper by the Wigner distribution function. Optical Engineering, 2001, 40, 1717.	1.0	0
80	Optical coherence tomography by spatio-temporal joint transform correlator. , 2000, 4087, 1282.		1
81	<title>Optical learning neural network with fuzzy controlling</title> . , 2000, 4089, 676.		1
82	<title>Pattern recognition neural-net by spatial mapping of biology visual field</title> . , 2000, , .		1
83	<title>Spatio-temporal joint pulse shaper: analysis of the property by Wigner distribution function</title> . , 2000, 4089, 836.		Ο
84	Time-space conversion of femtosecond light pulse by spatio-temporal joint transform correlator. Optics Communications, 2000, 177, 135-139.	2.1	4
85	Optical coherence tomography by spectral interferometric joint transform correlator. Optics Communications, 2000, 186, 51-56.	2.1	21
86	Terminal Attractor Optical Associative Memory for Pattern Recognition. Japanese Journal of Applied Physics, 2000, 39, 908-911.	1.5	8
87	Multilayer neural network with a fuzzy controlled learning method for optical pattern training. Optical Engineering, 2000, 39, 2734.	1.0	Ο
88	Improvement of the generalization capability for a pattern-recognition neural network that uses a Gaussian-synapse neuron model. Applied Optics, 2000, 39, 770.	2.1	2
89	Large-scale optical neural network with high-speed learning. , 1999, , .		0
90	Capacity of optical associative memory using a terminal attractor model. Optics Communications, 1998, 146, 49-54.	2.1	2

#	Article	IF	CITATIONS
91	Terminal attractor optical associative memory with adaptive control parameter. Optics Communications, 1998, 151, 353-365.	2.1	3
92	Optical learning neural network with a Pockels readout optical modulator. Applied Optics, 1998, 37, 2852.	2.1	9
93	Optical image transformations for fully parallel optical analog-to-digital conversion. Applied Optics, 1998, 37, 3607.	2.1	3
94	<title>Optical learning neural networks with two-dimensional structure</title> . , 1998, 3402, 226.		4
95	<title>Real-time face recognition system with optical learning neural network</title> . , 1998, 3466, 240.		0
96	Photon wall: three-dimensional control of femtosecond light pulse. , 1998, 3491, 700.		0
97	Simplification of Space-Variant Parallel Logic Operations Using the Temporal Method. Optical Review, 1997, 4, 305-308.	2.0	1
98	Method to Determine the Effective Group Refractive Index of an Optical Waveguide Using a Steplike Optical Frequency Sweep Generator. Japanese Journal of Applied Physics, 1995, 34, L526-L528.	1.5	0
99	Optical Learning Neural Network Using a Selfoc Microlens Array for Pattern Recognition. Optical Review, 1994, 1, 44-46.	2.0	5
100	Reversal-input superposing technique for all-optical neural networks. Applied Optics, 1994, 33, 1477.	2.1	8
101	<title>Renewal method of weight matrix in optical neural network</title> . , 1993, , .		2
102	Optical Learning Neural Network Using Selfoc Microlens Array. Japanese Journal of Applied Physics, 1992, 31, 1689-1693.	1.5	20
103	Binary logic operations using a beam-scanning laser diode. Optical Engineering, 1992, 31, 799.	1.0	1
104	<title>Recent research on optical neural networks in Japan</title> . , 1991, , .		0
105	Transverse Mode Characteristics of a DBR-Surface Emitting Laser with Buried Heterostructure. Japanese Journal of Applied Physics, 1991, 30, 3879-3882.	1.5	18
106	Optical Implementation of Semantic Networks Based on Association. Japanese Journal of Applied Physics, 1990, 29, L1321-L1324.	1.5	2
107	Beam Scanning Binary Logic. Japanese Journal of Applied Physics, 1990, 29, L1268-L1269.	1.5	2
108	Experimental Demonstration of Optical Three-Layer Neural Network. Japanese Journal of Applied Physics, 1990, 29, L1565-L1568.	1.5	17

#	Article	IF	CITATIONS
109	Diffusion Properties of Mg in AlxGa1-xAs. Japanese Journal of Applied Physics, 1989, 28, L1-L3.	1.5	5
110	Optical and electrical properties of C+-implanted GaAs. Nuclear Instruments & Methods in Physics Research B, 1989, 39, 457-460.	1.4	3
111	A theoretical explanation for the red energy shift of a newly discovered, exclusively acceptorâ€associated emission in GaAs. Journal of Applied Physics, 1987, 62, 1833-1836.	2.5	28
112	Liquidâ€phase epitaxy of heavily Mgâ€doped GaAs: Formation of a new nearâ€bandâ€edge emission exclusively pertinent to acceptor impurities. Journal of Applied Physics, 1987, 62, 3212-3215.	2.5	9
113	Photoluminescence of Mgâ€doped GaAs grown by molecular beam epitaxy using Mg3As2as a Mg source: A comparison with Mg+ion implantation. Applied Physics Letters, 1986, 49, 1184-1186.	3.3	32